

# A Hunt for Highly Charged Ions as Ultra-stable Optical Clock Candidates: Art of the energy level-crossing approach

<sup>a</sup>Yan-mei Yu\* and <sup>b</sup>B. K. Sahoo†

<sup>a</sup>*Beijing National Laboratory for Condensed Matter Physics,  
Institute of Physics, Chinese Academy of Sciences, Beijing 100190, China*

<sup>b</sup>*Atomic, Molecular and Optical Physics Division,  
Physical Research Laboratory, Navrangpura, Ahmedabad 380009, India*

(Dated: July 28, 2023)

We examine energy level-crossings of fine-structure (FS) levels in the heavier highly charged ions (HCIs) with  $d^6$  and  $d^8$  configurations. From the analysis, we find that some of these HCIs are tailor-made for atomic clocks with quality factors ranging from  $10^{16}$  to  $10^{18}$  and fractional uncertainties below  $10^{-19}$  level. Many of them are also realized to be highly sensitive to the observation of temporal variation of FS constant ( $\alpha$ ) and testing violation of local Lorentz symmetry invariance (LLI). To probe variations of  $\alpha$  and LLI, we have determined their corresponding sensitivity coefficients in the investigated HCIs. Similarly, we have estimated orders of magnitudes of the Zeeman, Stark, black-body radiation and electric quadrupole shifts of the clock transitions of the considered HCIs in order to demonstrate them as the potential candidates for atomic clocks.

Highly charged ion (HCI) as atomic clock using the magnetic dipole (M1) transition between the fine-structure (FS) splitting of the ground state in  $\text{Ar}^{13+}$  has been realized in laboratory [1]. The motivation to use  $\text{Ar}^{13+}$  as an ultra-precise optical clock was driven from the theoretical studies carried out earlier [2, 3]. Generally, the HCIs have enhanced sensitivity coefficients to variation of many fundamental physical constants and they show least response to external perturbations. These unique characteristics of HCIs make them potential candidates, when considered as optical clocks, as the finest sensors to test many fundamental postulates of modern quantum mechanics [4–6]. In view of these testings, it is essential to use heavier HCIs than  $\text{Ar}^{13+}$  ion for optical clocks. Also, improvement in the uncertainties of  $\text{Ar}^{13+}$  clock could be a challenge.

HCIs with large  $Q$  are particularly useful to overcome low signal-to-noise ratio and to improve the stability limit. For example, though  $\text{Ar}^{13+}$  has a relatively simple electronic structure, its milli-Hz clock linewidth impedes the clock stability. This could result in longer averaging time up to days to achieve the intended high accuracy. As outlined in Ref. [6], one of the most prevailing approaches to find out suitable atomic clock candidates is to analyze energy level-crossings (ELCs) in the isoelectronic HCIs. Historically, study of ELCs in atomic systems are interesting to fathom energy level shifting in the presence of external electromagnetic fields [7, 8]. In case of HCIs, this phenomena refers to the reordering of energy level positioning with the degree of ionization [9, 10]. By analyzing ELCs, a number of HCIs have been proposed as potential candidates for atomic clocks like  $\text{Ir}^{17+}$  [11],  $\text{Pr}^{9+}$  [12],  $\text{Cf}^{16+}$  and  $\text{Cf}^{17+}$  [13, 14],  $\text{Nd}^{9+}$  [15], etc.. Near ELCs, frequencies of atomic transitions can be within the optical range which can be used as frequency standards. Accurate prediction of energy level structures and their spectroscopic properties in these HCIs, especially those

are having multivalence electrons in the outer  $f$ -shell, are extremely difficult using available many-body methods.

In this Letter, we demonstrate a unique class of heavier HCIs as potential candidates for optical clocks having larger  $Q$  values with projected fractional uncertainties below  $10^{-19}$  level. These HCIs have  $(n = 4, 5)d^{6,8}$  electronic configurations giving rise to multiple FS splitting. By analyzing ELC of these FS levels (FS-ELC) with the increasing values of atomic number ( $Z$ ) and ion charge ( $Z_{\text{ion}}$ ) along an isoelectronic sequence, we shortlist a few selective HCIs possessing at least two optical-accessible clock transitions. Simultaneous interrogation of two clock transitions in a given atomic system may be useful to minimize systematic uncertainties in clock experiments like in  $\text{Yb}^+$  [16] to probe variation of FS constant ( $\alpha$ ). Moreover, the clock transitions in these HCIs show negative differential values for dipole polarizabilities ( $\alpha^{E1}$ ) suggesting that these ions can also be advantageous for undertaking in the multi-ion clock scheme [17, 18]. Owing to relatively simpler energy level structures compared to many proposed heavier HCI clock candidates, the shortlisted candidates are easier to interrogate in the experiment and it is possible to carry out calculations of their spectroscopic properties using the available state-of-the-art many-body methods. The clock transitions in these HCIs also show reasonably enhanced sensitivity coefficients for testing local Lorentz symmetry invariance (LLI) and probing variation of  $\alpha$ . To demonstrate low systematic effects in the clock frequency measurements, we have estimated major systematic effects due to the Zeeman, Stark, black-body radiation (BBR), and electric quadrupole shifts by considering typical orders of field strengths.

To find out the energy level positioning of ions with  $d^{6,8}$  configurations for laser trapping and interrogation purpose, we have employed three independent first-principle many-body methods to calculate excitation en-

TABLE I: Comparison of experimental (Exp.) and calculated values of excitation energies (in  $\text{cm}^{-1}$ ) of the fine-structure levels in the Cr-like, Fe-like, Mo-like, W-like and Ru-like HCIs with  $d^6$  and  $d^8$  configurations. Calculations are carried out at the CI+MBPT, CCSD, CISD, and CISDT method approximations but results from the CISDT method are considered as our final theoretical results for which differences from the Exp. values [19, 20] are given as Diff. in percentage.

Level	Exp.	CI+MBPT	CCSD	CISD	CISDT	Diff.(%)
Cr-like $\text{Zn}^{6+}$ with $3d^6$ $^5D_4$ ground state [19]						
$^5D_3$	1567	1595		1559	1572	0.3
$^5D_2$	2579	2633		2586	2584	0.2
$^5D_1$	3230	3294		3239	3226	-0.1
$^5D_0$	3542	3621		3557	3537	-0.1
Fe-like $\text{Rb}^{11+}$ with $3d^8$ $^3F_4$ ground state [19]						
$^3F_3$	10980	10980	10772	11276	11285	2.8
$^3F_2$	15610	15796	15468	16278	15978	2.4
$^1D_2$	34020	35410	34571	37159	35284	3.7
$^3P_1$	46580	48774	46748	50590	48642	4.4
$^3P_0$	47220	49417	47318	51362	49130	4.0
$^3P_2$	48070	49654	48731	52037	50034	4.1
Mo-like $\text{Pd}^{4+}$ with $4d^6$ $^5D_4$ ground state [20]						
$^5D_3$	2103.8	2167		2106	2136	1.6
$^5D_2$	3175.3	3330		3259	3239	2.0
$^5D_1$	3950.0	4141		4053	4027	1.9
$^5D_0$	4306.4	4526		4429	4391	2.0
W-like $\text{Pt}^{4+}$ with $5d^6$ $^5D_4$ ground state [19]						
$^5D_2$	6026.34	6712		6720	6337	5.2
$^5D_3$	7612.63	7576		7210	7412	-2.6
$^5D_0$	10817.6	11378		11216	10893	0.7
$^5D_1$	10826.8	11085		10797	10756	-0.7
Ru-like $\text{Xe}^{10+}$ with $4d^8$ $^3F_4$ ground state [19]						
$^3F_2$	13140.	13488	13453	14250	13322	1.4
$^3F_3$	15205.	14986	15472	15490	15114	-0.6
$^3P_2$	26670.	26934	27172	27884	26812	0.5
$^3P_0$	32210.	33192	32924	34715	32637	1.3
$^3P_1$	34610.	35396	35225	36462	34879	0.8

ergies (EE). We have adopted the following procedure to ensure about validity of these calculations. First, we consider a representative HCI of a given isoelectronic sequence, for which experimental values are available, to identify their ground and excited state configurations. Then, different many-body methods are employed to reproduce the EEs and cross-verify among them. The initial ions under investigations are Cr-like  $\text{Zn}^{6+}$ , Fe-like  $\text{Rb}^{11+}$ , Mo-like  $\text{Pd}^{4+}$ , Ru-like  $\text{Xe}^{10+}$ , and W-like  $\text{Pt}^{4+}$ . Both the experimental values [19, 20] and calculations from three independent methods of EEs of these HCIs are given in Table I. We employ first the combined configuration interaction method and many-body perturbation theory (CI+MBPT) using AMBiT code [21] in which

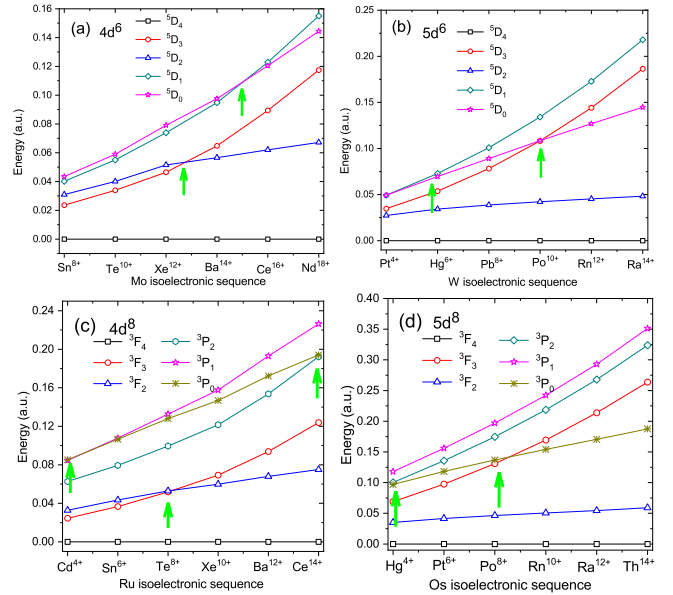


FIG. 1: Plots showing FS-ELCs (pointed out by arrows) in HCIs with the  $(n = 4, 5)d^{6,8}$  configurations of the (a) Mo-like, (b) W-like, (c) Ru-like, and (d) Os-like isoelectronic sequences. Energies are given in atomic units (a.u.).

correlations among the valence electrons from the  $n(= 3, 4, 5)d^{6,8}$  orbitals are treated explicitly at the singles and doubles excitation approximation in the CI method and correlations among the valence electrons and the atomic core are accounted for using the MBPT method. We find good agreement between the CI+MBPT results and the experimental data for the systems with  $n = 3$ , but large differences are seen for the ions with  $n = 4, 5$ . Next, we adopt the singles and doubles approximated Fock-space coupled-cluster theory (CCSD method) [22] implemented in the DIRAC program [23] to obtain the FS among the states with  $nd^8$  configurations by detaching two electrons from the closed-core  $nd^{10}$ . The CCSD results show similar accuracy with the CI+MBPT results. Then, we applied the multi-reference configuration interaction method with the singles and doubles excitations (CISD method) followed by singles, doubles, and triples excitations (CISDT method) in the general active space scheme [24–26] that are implemented in the DIRAC program [23, 27]. In both the CISD and CISDT methods, electrons only from the valence  $nd$  shells and from the  $(n-1)s, p$  shells are allowed in the excitation processes. In most of heavier HCIs, the CISDT results are found to be better in agreement with the experimental values than the CI+MBPT and CCSD results. Thus, results from the CISDT method, that incorporates more physical effects through the triple excitations than the CISD method, are considered as the final calculated values. Nonetheless, comparative computations using all the three considered many-body methods helped us to

TABLE II: Trends of FS splitting energies (in  $\text{cm}^{-1}$ ) in different isoelectronic sequences of the HCIs with the  $n(= 4, 5)d^{6,8}$  configurations using the CISDT method. ELCs occurring for the HCIs are highlighted by bold fonts.

Mo-like	$4d^6$ $^5D_4$ ground state					
	Sn <sup>8+</sup>	Te <sup>10+</sup>	Xe <sup>12+</sup>	Ba <sup>14+</sup>	Ce <sup>16+</sup>	Nd <sup>18+</sup>
$^5D_3$	5161	7441	10190	14223	19619	25759
$^5D_2$	6792	8788	11308	<b>12412</b>	<b>13609</b>	<b>14735</b>
$^5D_1$	8817	12062	16215	20807	26969	34017
$^5D_0$	9543	12937	17357	21412	<b>26444</b>	<b>31706</b>
W-like	$5d^6$ $^5D_4$ ground state					
	Pt <sup>4+</sup>	Hg <sup>6+</sup>	Pb <sup>8+</sup>	Po <sup>10+</sup>	Rn <sup>12+</sup>	Ra <sup>14+</sup>
$^5D_3$	7412	11792	17160	23749	31649	40925
$^5D_2$	<b>6637</b>	<b>7553</b>	<b>8488</b>	<b>9261</b>	<b>9944</b>	<b>10617</b>
$^5D_1$	10756	16002	22124	29425	37949	47811
$^5D_0$	10893	<b>15271</b>	<b>19546</b>	<b>23814</b>	<b>27867</b>	<b>31777</b>
Ru-like	$4d^8$ $^3F_4$ ground state					
	Cd <sup>4+</sup>	Sn <sup>6+</sup>	Te <sup>8+</sup>	Xe <sup>10+</sup>	Ba <sup>12+</sup>	Ce <sup>14+</sup>
$^3F_3$	5378	8034	11378	15114	20573	27182
$^3F_2$	7189	9526	11594	<b>13322</b>	<b>14933</b>	<b>16471</b>
$^3P_2$	13775	17424	21827	26812	33724	42210
$^3P_1$	18584	23658	29127	34879	42360	49661
$^3P_0$	18717	<b>23402</b>	<b>28074</b>	<b>32637</b>	<b>37821</b>	<b>42610</b>
Os-like	$5d^8$ $^3F_4$ ground state					
	Hg <sup>4+</sup>	Pb <sup>6+</sup>	Po <sup>8+</sup>	Rn <sup>10+</sup>	Ra <sup>12+</sup>	Th <sup>14+</sup>
$^3F_3$	15142	21409	28721	37189	46908	57897
$^3F_2$	<b>7732</b>	<b>9104</b>	<b>10170</b>	<b>11096</b>	<b>11960</b>	<b>12953</b>
$^3P_2$	21996	29778	38349	47965	58781	71044
$^3P_1$	25876	34245	43202	53149	64286	77057
$^3P_0$	<b>21296</b>	<b>25957</b>	<b>30041</b>	<b>33816</b>	<b>37407</b>	<b>41165</b>

test reliability of the calculations.

We analyze the FS-ELCs of the aforementioned isoelectronic sequence HCIs with  $nd^6$  and  $nd^8$  configurations for  $n = 3, 4$  and  $5$  by increasing ionization number  $Z_{\text{ion}}$ . We focus mainly on the heavier HCIs with moderate values of  $Z_{\text{ion}}$  lying in the range 4-20 that can be produced using table-top electron ion beam facility. Furthermore, we concentrate excited states within the range of 300-1000nm that can be easily accessible by the available lasers. The radioactive HCIs with  $n(= 6)d^{6,8}$  configurations having half-lifetimes shorter than seconds are not investigated because they will not be suitable to consider in the laboratory for making clocks. The EEs between the FS splitting in the  $n(= 4, 5)d^{6,8}$  isoelectronic sequences are shown in Fig. 1. The  $n(= 3)d^{6,8}$  isoelectronic sequences are not shown since no ELCs are found for them. Quantitative data for EEs are tabulated in Table II from the CISDT method. Since the Mo-like and W-like isoelectronic sequences have  $n(= 4, 5)d^6$  configurations, they will have low-lying FS levels as  $^5D_J$  for  $J = 0, 1, 2, 3, 4$ . It can be seen from Fig. 1(a) that for

smaller  $Z_{\text{ion}}$  values in the Mo-like isoelectronic sequences, such as from Sn<sup>8+</sup> to Xe<sup>12+</sup>, the FS level ordering follows as  $J = 4, 3, 2, 1, 0$ . For increasing  $Z_{\text{ion}}$  value, the  $^5D_3$  and  $^5D_2$  levels swap the ordering around Ba<sup>12+</sup> and the  $^5D_0$  level moves downwards to be below the  $^5D_1$  level around Ce<sup>16+</sup>. Thus, it shows ELCs between the  $J = 2$  and  $J = 3$  levels then between the  $J = 0$  and  $J = 1$  levels as indicated by arrows in Fig. 1(a) and shown in bold fonts in Table II. The W-like isoelectronic sequences also show similar ELCs, as shown in Fig. 1(b) and in the above table. The Ru-like and the Os-like isoelectronic sequences are found to have FS splitting as  $^3F_2, ^3F_1, ^3F_0, ^3P_2, ^3P_1$ , and  $^3P_0$  for lower  $Z_{\text{ion}}$  values, but these ordering changes from  $^3F_3$  to  $^3F_2$ , from  $^3P_1$  to  $^3P_0$ , then from  $^3P_0$  to  $^3F_3$  as shown by arrows in Figs. 1(c) and (d) for which data are quoted in Table II.

After understanding ELCs in different isoelectronic systems investigated here, we now intend to use this knowledge in identifying potential candidates for atomic clocks. We find at least two clock transitions in each type of isoelectronic HCIs showing ELCs, which are named as Clock-I and Clock-II for further discussions. In HCIs with  $nd^6$  configurations, the  $^5D_4 - ^5D_2$  and  $^5D_4 - ^5D_0$  ELC transitions basically correspond to the Clock-I and Clock-II transitions respectively. Similarly, the  $^3F_4 - ^3F_2$  and  $^3F_4 - ^3P_0$  ELC transitions in the ions with the  $nd^8$  configurations can be the Clock-I and Clock-II transitions respectively. Since these forbidden transitions are mainly guided by the electric quadrupole (E2) decay channel, they are expected to be quite narrow leading to very long lifetime for the excited states. We have verified this by estimating the decay rates and lifetimes of the excited states. In Table III, we list a number of HCIs that have Clock-I and Clock-II transitions in the wavelength ( $\lambda$ ) around 300-1000 nm. We provide the  $\lambda$  values and  $Q$  values of the clock transitions and lifetimes ( $\tau$ ) of the excited states associated with both the clock transitions. As can be noticed from this table, the  $\tau$  and  $Q$  values in almost all the listed HCIs are sufficiently large. This essentially advocates that they all are apt for making ultra-stable optical clocks, but we have highlighted some of the HCIs in bold fonts in the above table which, we feel, have overall advantages for clocks in view of laboratory consideration and probing fundamental physics.

The  $\alpha$ -variation sensitivity coefficients are defined as

$$K_\alpha = 2(q_2 - q_1)/h\nu, \quad (1)$$

where  $q_{1/2}$  are  $\alpha$ -variation sensitivity coefficients of the ground and excited states of the clock transition respectively,  $h$  is the Plank constant, and  $\nu$  is the clock frequency. The  $K_\alpha$  values of the proposed clock transitions presented in Table III show that they are comparable or larger than the  $^{171}\text{Yb}$  clock transitions [28]. Similarly,

TABLE III: The estimated  $\lambda$ ,  $\tau$ ,  $Q$ ,  $\Delta R$ , and  $\langle J||\mathbf{T}^{(2)}||J\rangle$  values for the identified Clock-I and Clock-II transitions through ELC in a large number of HCIs. The  $\langle J||\mathbf{T}^{(2)}||J\rangle$  values for the ground and excited states of the only Clock-I transition are given for representation. See text for definitions of notations.  $a[b]$  denotes  $a \times 10^b$ .

	Clock-I					Clock-II					$\langle J  \mathbf{T}^{(2)}  J\rangle$ (a.u.)	
	$\lambda$ (nm)	$\tau$ (s)	$Q$	$K_\alpha$	$\Delta R$	$\lambda$ (nm)	$\tau$ (s)	$Q$	$K_\alpha$	$\Delta R$	Ground	Excited
Mo-like	$4d^6$											
<b>Nd<sup>18+</sup></b>	<b>679</b>	<b>860</b>	2.4[18]	<b>0.1</b>	<b>0.8</b>	<b>315</b>	<b>138</b>	8.2[17]	<b>1.5</b>	<b>2.1</b>	<b>147</b>	-47.5
W-like	$5d^6$											
Hg <sup>6+</sup>	1255	1889	2.8[18]	0.4	1.7	655	505	1.5[18]	1.7	3.3	51.2	-14.6
Pb <sup>8+</sup>	1178	1250	2.0[18]	0.5	1.2	512	107.0	3.9[17]	1.3	2.5	62.2	-20.8
Po <sup>10+</sup>	1080	967	1.7[18]	-0.1	1.1	420	32.9	1.5[17]	1.1	2.1	73.5	-27.9
<b>Rn<sup>12+</sup></b>	<b>1006</b>	<b>810</b>	1.4[19]	<b>-0.04</b>	<b>0.9</b>	<b>359</b>	<b>13.5</b>	7.1[16]	<b>0.9</b>	<b>1.8</b>	<b>85.5</b>	<b>-36.0</b>
Ra <sup>14+</sup>	942	690	1.3[18]	-0.01	0.9	315	6.8	4.1[16]	0.8	1.6	98.0	-44.7
Ru-like	$4d^8$											
Te <sup>8+</sup>	863	772	1.7[18]	0.7	1.4	356	14	7.2[16]	0.5	1.3	-41.7	15.3
<b>Xe<sup>10+</sup></b>	<b>761</b>	<b>480</b>	1.2[18]	<b>0.4</b>	<b>1.0</b>	<b>310</b>	<b>9.3</b>	5.6[16]	<b>0.5</b>	<b>1.3</b>	-52.1	<b>31.6</b>
Ba <sup>12+</sup>	670	285	8.0[17]	0.2	0.9	264	5.1	3.6[16]	0.5	1.2	-63.5	46.8
Os-like	$5d^8$											
Hg <sup>4+</sup>	1293	643	9.4[18]	-0.3	1.8	470	8.2	3.3[16]	0.3	2.4	-27.8	23.4
<b>Pb<sup>6+</sup></b>	<b>1098</b>	<b>393</b>	6.7[18]	<b>-0.3</b>	<b>1.5</b>	<b>385</b>	<b>3.8</b>	1.9[16]	<b>0.3</b>	<b>1.9</b>	-36.7	<b>31.5</b>
Po <sup>8+</sup>	983	311	6.0[18]	-0.1	1.2	333	2.3	1.3[16]	0.3	1.5	-46.7	40.3
Rn <sup>10+</sup>	901	268	5.6[19]	-0.1	1.1	296	1.6	1.0[16]	0.3	1.4	-57.3	49.2

the LLI interaction Hamiltonian is given by [29]

$$H^{LLI} = -C_0^{(0)} \frac{\mathbf{p}^2}{2m_e} - C_0^{(2)} \frac{\mathbf{T}^{(2)}}{6m_e}, \quad (2)$$

where  $m_e$  is the mass of an electron,  $C_0^{(0/2)}$  are related to LLI violating coefficients,  $\mathbf{p}$  is the momentum operator and  $\mathbf{T}^{(2)}$  is a second-rank tensor. Therefore, enhancement of LLI in an atomic transition depends on the kinetic energy (K.E.) and sensitivity of the  $\mathbf{T}^{(2)}$  operator in the states involved. Enhancement due to K.E. of electrons are defined as  $\Delta R = -(\langle J||\mathbf{p}^2||J\rangle_2 - \langle J||\mathbf{p}^2||J\rangle_1)/(2h\nu)$ , while  $\mathbf{T}^{(2)}$  are estimated by the expectation values. Clock-I transitions highlighted in Table III show very large differential values for  $\Delta R$  and expectation values of the  $\mathbf{T}^{(2)}$  operator. Though these values are slightly smaller than the octupole transition of Yb<sup>+</sup> [30], but they are much larger than the clock transitions of Ca<sup>+</sup> [31] and Sr<sup>+</sup> [32]. It indicates that the proposed clock transitions are not only suitable to be considered for ultra-precise clocks they are also very sensitive to probe LLI violation.

Next, we discuss the major systematic effects in the clock transitions of a few representative Nd<sup>18+</sup>, Rn<sup>12+</sup>, Xe<sup>10+</sup>, and Pb<sup>6+</sup> HCIs as these effects are of almost similar orders in other considered HCIs. Among these, it would be easier to consider the Xe<sup>10+</sup> ion in the laboratory as proof-of-principle for measuring its energy levels are already demonstrated. To estimate typical orders shifts due to electric fields and BBR shifts in the

above HCIs, we have determined scalar ( $\alpha_0^{E1}$ ) and tensor ( $\alpha_2^{E1}$ ) components of  $\alpha^{E1}$ , and E2 moments ( $\Theta$ ) of the ions using the CISDT method in the finite-field (FF) approach. As seen in Table IV, the  $\delta\alpha_0^{E1}$  values are around  $10^{-3} - 10^{-4}$ . It means that the fractional differential Stark shifts,  $\delta E_{Stark} = -\delta\alpha_0^{E1}\mathcal{E}^2/2$ , of the clock transitions in the above HCIs, for a typical electric field strength  $\mathcal{E}=10$  V/m, can be negligibly small. Contributions from the  $\alpha_2^{E1}$  values can be minimized by choosing suitable quantization axis while carrying out the measurements. Also for such small  $\delta\alpha_0^{E1}$  values, the BBR shifts can be suppressed far below  $10^{-19}$  in the cryogenic environments. The excited state of Clock-II transition in Rn<sup>12+</sup> has negative  $\delta\alpha_0^{E1}$  value, which can help in producing ‘‘magic’’ trap drive frequency,  $\Omega$ , as mentioned in Ref. [33] and estimated to be  $\Omega \approx 2\pi \times 520$  MHz. The electric quadrupole shift, given by  $\Delta E_{Quad} = -\Theta\mathcal{E}_{zz}/2$  with  $\mathcal{E}_{zz}$  is the gradient of the applied electric field in the  $z$ -direction, found to be around  $10^{-14} - 10^{-15}$  in the above HCIs. It is possible to nullify uncertainties due to these shifts by performing frequency measurements in all azimuthal  $M$ -components and considering the averaged frequency. We have also determined the Lande  $g_J$ -factors and the scalar M1 polarizabilities ( $\alpha_0^{M1}$ ) in the expectation value approach using the CISDT method. The  $g_J$  values will be useful for calibrating the magnetic field strengths ( $B$ ) during the measurements. The first-order Zeeman shifts can be eliminated by choosing the  $M_J = 0 \rightarrow M_J = 0$  transitions

TABLE IV: A summary of properties relevant to systematic effects estimation for the clock states of a few representative HCIs evaluated using the CISDT method.

Items	Nd <sup>18+</sup>	Rn <sup>12+</sup>	Xe <sup>10+</sup>	Pb <sup>6+</sup>
<u>Level configurations</u>				
Ground state	4d <sup>6</sup> 5D <sub>4</sub>	5d <sup>6</sup> 5D <sub>4</sub>	4d <sup>8</sup> 3F <sub>4</sub>	5d <sup>8</sup> 3F <sub>4</sub>
Clock-I state	4d <sup>6</sup> 5D <sub>2</sub>	5d <sup>6</sup> 5D <sub>2</sub>	4d <sup>8</sup> 3F <sub>2</sub>	5d <sup>8</sup> 3F <sub>2</sub>
Clock-II state	4d <sup>6</sup> 5D <sub>0</sub>	5d <sup>6</sup> 5D <sub>0</sub>	4d <sup>8</sup> 3F <sub>0</sub>	5d <sup>8</sup> 3F <sub>0</sub>
<u>Lande g<sub>J</sub>-factors</u>				
Ground state	1.4068	1.3387	1.2421	1.2351
Clock-I state	1.406	1.3492	0.9994	1.1171
<u>Θ values in a. u.</u>				
Ground state	0.1088	0.2356	-0.1190	0.2828
Clock-I	-0.0326	-0.1108	0.0674	0.2011
<u>α<sub>0</sub><sup>E1</sup> values in a.u.</u>				
Ground state	0.2196	0.8067	0.5817	2.4427
Clock-I state	0.2203	0.8099	0.5824	2.4495
Clock-II state	0.2196	0.8042	0.5826	2.4540
<u>δα<sub>0</sub><sup>E1</sup> values in a.u.</u>				
Clock-I transition	0.0007	0.0032	0.0007	0.0069
Clock-II transition	0.0001	-0.0025	0.0009	0.0113
<u>α<sub>2</sub><sup>E1</sup> values in a.u.</u>				
Ground state	0.0047	-0.0021	0.0036	0.0549
Clock-I state	-0.0015	0.0031	-0.0057	-0.0291
<u>α<sup>M1</sup> values in a.u.</u>				
Ground state	-5.5×10 <sup>4</sup>	-3.8×10 <sup>4</sup>	-5.7×10 <sup>4</sup>	-5.5×10 <sup>4</sup>
Clock-I state	-2.9×10 <sup>5</sup>	-1.1×10 <sup>5</sup>	-3.0×10 <sup>5</sup>	-6.4×10 <sup>4</sup>
Clock-II state	-4.8×10 <sup>6</sup>	-4.5×10 <sup>5</sup>	-2.1×10 <sup>6</sup>	-5.3×10 <sup>5</sup>

or adopting the averaging frequency measurement technique. The second-order Zeeman shift can be estimated by  $\delta E_{Zeem}^{(2)} = -\frac{1}{2}\delta\alpha^{M1}B^2$ , where  $\delta\alpha^{M1}$  is the differential  $\alpha^{M1}$  values for the clock transitions. Assuming a typical magnetic field strength of  $B = 5 \times 10^{-8}$ T, the fractional frequency shifts,  $\delta E_{Zeem}^{(2)}/\nu$ , are found to be below  $10^{-19}$ . Thus, the aforementioned discussions suggest that the fractional uncertainties to the proposed Clock-I and Clock-II transitions in the investigated HCIs can be  $10^{-19}$  level. Nonetheless, some of these systematic effects can be further reduced by selecting transitions among hyperfine levels of the clock states appropriately.

In Summary, we have identified a large number of heavier highly charged ions by analyzing energy level-crossings of the fine-structure splitting of the ground  $d^6$  and  $d^8$  open-shell configurations that are advantageous for making ultra-stable and high-precision optical atomic clocks. They offer at least two set of clock transitions with quality factors about  $10^{16-18}$  and fractional uncertainties due to major systematics effects are below  $10^{-19}$  level compared to the currently undertaken Ar<sup>13+</sup> clock transition. These clock transitions also show very sensitive for probing fundamental phenomena like possible

temporal variation of the fine structure constant and local Lorentz symmetry invariance.

YY thanks K. Yao for sharing the work of the 3d ion EBIT spectroscopy. This work is supported by The National Key Research and Development Program of China (2021YFA1402104), and Project supported by the Space Application System of China Manned Space Program. BKS would like to acknowledge use of ParamVikram-1000 HPC of Physical Research Laboratory (PRL), Ahmedabad.

\* Electronic address: ymyu@aphy.iphy.ac.cn

† Electronic address: bijaya@prl.res.in

- [1] S. A. King, L. J. Spieß, P. Micke, A. Wilzewski, T. Leopold, E. Benkler, R. Lange, N. Huntemann, A. Surzhykov, V. A. Yerokhin, J. R. Crespo López-Urrutia, P. O. Schmidt, Nature **611**, 43 (2022).
- [2] V. I. Yudin, A. V. Taichenachev, and A. Derevianko, Phys. Rev. Lett. **113**, 233003 (2014).
- [3] Y. M. Yu and B. K. Sahoo, Phys. Rev. A **99**, 022513 (2019).
- [4] M. S. Safronova, D. Budker, D. DeMille, Derek F. Jackson Kimball, A. Derevianko, and C. W. Clark, Rev. Mod. Phys. **90**, 025008 (2018).
- [5] M. G. Kozlov, M. S. Safronova, J. R. Crespo Lopez-Urrutia, and P. O. Schmidt, Rev. Mod. Phys. **90**, 045005 (2018).
- [6] Y. M. Yu, B. K. Sahoo, and B. B. Suo, Front. Phys. **11**, 1104848 (2023).
- [7] R. T. RoszcoE, Phys. Rev **138**, A22, (1965).
- [8] J. S. Levine, P. A. Bonczyk, and A. Javan, Phys. Rev. Lett. **22**, 267 (1969).
- [9] J. C. Berengut, V. A. Dzuba, and V.V. Flambaum, Phys. Rev. Lett. **105**, 120801 (2010).
- [10] J. C. Berengut, V. A. Dzuba, V. V. Flambaum, and A. Ong, Phys. Rev. A **86**, 022517 (2012).
- [11] J. C. Berengut, V. A. Dzuba, V.V. Flambaum, and A. Ong, Phys. Rev. Lett. **106**, 210802 (2011).
- [12] H. Bekker, A. Borschevsky, Z. Harman, C. H. Keitel, T. Pfeifer, P. O. Schmidt, J. R. Crespez-Urrutia, J. C. Berengut, Nat. Commun. **10**, 5651 (2019).
- [13] J. C. Berengut, V. A. Dzuba, V.V. Flambaum, and A. Ong, Phys. Rev. Lett. **109**, 070802 (2012).
- [14] S. G. Porsev, U. I. Safronova, M. S. Safronova, P. O. Schmidt, A. I. Bondarev, M. G. Kozlov, I. I. Tupitsyn, and C. Cheung, Phys. Rev. A **102**, 012802 (2020).
- [15] Y. M. Yu, P. Duo, S. L. Chen, B. Arora, H. Guan, K. Gao, and J. Chen, Atoms **10**, 123 (2022).
- [16] R. Lange, N. Huntemann, J. M. Rahm, C. Sanner, H. Shao, B. Lipphardt, Chr. Tamm, S. Weyers, and E. Peik, Phys. Rev. Lett. **126**, 011102 (2021).
- [17] K. Arnold, E. Hajiyev, E. Paez, C. H. Lee, M. D. Barrett, and J. Bollinger, Phys. Rev. A **92**, 032108 (2015).
- [18] Y. Huang, H. Guan, C. Li, H. Zhang, B. Zhang, M. Wang, L. Tang, T. Shi, and K. Gao, unpublished (arXiv 2022.07828 (2015)).
- [19] A. Kramida, Y. Ralchenko, J. Reader, and NIST ASD Team <https://physics.nist.gov/asd>.
- [20] A.J.J. Raassen and Th. A. M. van Kleef, Physica C **142**,

- 359 (1986).
- [21] E. V. Kahl and J. C. Berengut, *Comp. Phys. Comm.* **238**, 232 (2019).
- [22] L. Visscher, E. Eliav, and U. Kaldor, *J. Chem. Phys.* **115**, 9720 (2001).
- [23] DIRAC, a relativistic ab initio electronic structure program, Release DIRAC22 (2022), written by H. J. Aa. Jensen, et al. (available at <http://dx.doi.org/10.5281/zenodo.6010450>, see also <http://www.diracprogram.org>).
- [24] T. Fleig, J. Olsen and C. M. Marian, *J. Chem. Phys.* **114**, 4775 (2001).
- [25] T. Fleig and J. Olsen and L. Visscher, *J. Chem. Phys.* **119**, 2963 (2003).
- [26] T. Fleig and H. J. A. Jensen and J. Olsen and L. Visscher, *J. Chem. Phys.* **124**, 104106 (2006).
- [27] S. Knecht, H. J. A. Jensen, and T. Fleig, *J. Chem. Phys.* **128**, 014108 (2008).
- [28] Z. M. Tang, Y. M. Yu, B. K. Sahoo, C. Z. Dong, Y. Yang, and Y. Zou, *Phys. Rev. A* **107**, 053111 (2023).
- [29] M. A. Hohensee, N. Leefer, D. Budker, C. Harabati, V. A. Dzuba, and V. V. Flambaum, *Phys. Rev. Lett.* **111**, 050401 (2013).
- [30] V. A. Dzuba, V. V. Flambaum, M. S. Safronova, et al., *Nat. Phys.* **12**, 465 (2016).
- [31] B. K. Sahoo, *Phys. Rev. A* **99**, 050501(R) (2019).
- [32] R. Shaniv, R. Ozeri, M. S. Safronova, S. G. Porsev, V. A. Dzuba, V. V. Flambaum, and H. Häffner *Phys. Rev. Lett.* **120**, 103202 (2018)
- [33] P. Dubé, A. A. Madej, Z. Zhou, and J. E. Bernard, *Phys. Rev. A* **87**, 023806 (2013).